

UCLA

UCLA Previously Published Works

Title

Synthesis of ent-Ketorfanol via a C-H Alkenylation/Torquoselective 6 π Electrocyclization Cascade

Permalink

<https://escholarship.org/uc/item/2mm4p0n2>

Journal

Angewandte Chemie International Edition, 54(41)

ISSN

1433-7851

Authors

Phillips, Eric M
Mesganaw, Tehetena
Patel, Ashay
[et al.](#)

Publication Date

2015-10-05

DOI

10.1002/anie.201505604

Peer reviewed



Published in final edited form as:

Angew Chem Int Ed Engl. 2015 October 5; 54(41): 12044–12048. doi:10.1002/anie.201505604.

Synthesis of *ent*-Ketorfanol via a C–H Alkenylation/Highly Torquoselective 6π -Electrocyclization Cascade

Eric M. Phillips^[a], Tehetena Mesganaw^[a], Ashay Patel^[b], Simon Duttwyler^[a], Brandon Q. Mercado^[a], Kendall N. Houk^[b], and Prof. Dr. Jonathan A. Ellman^[a]

Kendall N. Houk: houk@chem.ucla.edu; Jonathan A. Ellman: jonathan.ellman@yale.edu

^[a]Department of Chemistry, Yale University, 225 Prospect St., New Haven, CT 06520 (USA)

^[b]Department of Chemistry and Biochemistry, University of California, Los Angeles, Los Angeles, CA 90095-1569 (USA)

Abstract

The asymmetric synthesis of *ent*-ketorfanol from simple and commercially available precursors is reported. A Rh(I)-catalyzed intramolecular C–H alkenylation/highly torquoselective 6π -electrocyclization cascade provides a fused bicyclic 1,2-dihydropyridine as a key intermediate. Computational studies were performed to understand the high torquoselectivity of the key 6π electrocyclization. Computations demonstrate a conformational effect is responsible for the observed selectivity. The ketone functionality and final ring are introduced in a single step by a redox neutral acid-catalyzed rearrangement of a vicinal diol to the requisite carbonyl followed by intramolecular Friedel–Crafts alkylation.

Keywords

heterocycles; alkaloids; asymmetric synthesis; C–H activation; torquoselectivity

Oxycodone¹ and related semisynthetic opioid ligands are effective and pervasively used medications for the management of pain. However, these compounds have significant liabilities that include dependency, tolerance, which results in increasing doses being required to maintain efficacy, and serious side effects of higher doses, such as respiratory failure. The very recent high resolution structures of a number of opioid receptor ligands in complex with several receptor sub-types provides an exceptional opportunity for the structure-based design of new opioid ligands with reduced liabilities.² However, access to different structural variants is constrained by reported synthetic routes to the approved semisynthetic opioid ligands, which rely on morphine, thebaine and other morphinoid natural products as heavily functionalized starting materials.^{3,4}

Our recently developed Rh-catalyzed C–H-functionalization/ 6π -electrocyclization cascade⁵ should enable direct and rapid entry to this important class of alkaloids from readily available achiral precursors. Herein, we demonstrate this approach with the asymmetric

Correspondence to: Kendall N. Houk, houk@chem.ucla.edu; Jonathan A. Ellman, jonathan.ellman@yale.edu.

Supporting information for this article is given via a link at the end of the document.

Author Manuscript

Author Manuscript

Author Manuscript

synthesis of *ent*-ketorfanol (**1**), the nonregulated enantiomer of the semisynthetic opioid drug ketorfanol (Scheme 1). *ent*-Ketorfanol should be accessible by the acid-catalyzed intramolecular Friedel–Crafts cyclization of intermediate **2**.⁶ This intermediate could possibly be obtained *in situ* from **3** under the acidic reaction conditions via a more speculative redox neutral process⁷ proceeding by ionization of the allylic oxygen functionality followed by a hydrogen shift (*vide infra*). Fused bicyclic tetrahydropyridine **3** would then be obtained by reduction of dihydropyridine **4** under mildly acidic reductive amination conditions. In the key step, bicyclic intermediate **4** should be accessible via an intramolecular Rh-catalyzed syn C-H bond addition to the alkyne followed by electrocyclization, which should hopefully proceed with high torquoselectivity due to remote asymmetric induction provided by the isopropylidene protected diol.^{8,9,10} The precursor for this cascade reaction, imine **6**, should be readily accessible from ester **7** through straightforward functional group transformations. Ester **7** should be obtainable by regioselective Sharpless asymmetric dihydroxylation,¹¹ isopropylidene protection, and alkyne benzylation of the achiral dienoate **8**.

The synthesis commenced with Swern oxidation of 4-pentyn-1-ol (**9**) and subsequent Horner–Wadsworth–Emmons reaction (Scheme 2) to furnish dienoate **10** (60% yield, 2 steps). A highly regio- and enantioselective Sharpless asymmetric dihydroxylation was performed on the olefin distal to the ester (81% yield, 95% *ee*).¹¹ Diol **11** was immediately protected using 2,2-dimethoxypropane and *p*TsOH to furnish acetonide **12** in 94% yield. X-ray structural analysis of **11** was also carried out to confirm that its absolute configuration was consistent with that predicted for AD-mix- α .¹²

Alkyne **12** was next benzylated by Cu(I)-mediated coupling to give a moderate yield of product **13** (50–70%).¹³ However, this process was plagued by long reaction times (4 days), the need for stoichiometric Cu(I), and difficulty in obtaining pure material. Ultimately, the efficient Pd-catalyzed method developed by Buchwald and co-workers¹⁴ enabled the coupling of benzyl chloride and terminal alkyne **12** in 75% yield (Scheme 2). DIBAL reduction and Dess–Martin periodinane oxidation afforded α,β -unsaturated aldehyde **14** (54% yield, 2 steps). Condensation with cyclopropylmethyl amine gave our key imine substrate **15** in 95% yield.

Author Manuscript

Author Manuscript

With α,β -unsaturated imine **15** in hand, we attempted the crucial tandem Rh(I)-catalyzed intramolecular alkenylation/ 6π -electrocyclization (Scheme 3).⁵ Notably, while previously reported examples of diastereoselective electrocyclizations of azatrienes rely on stereogenic centers directly attached to the two atoms involved in ring closure,^{8–10} azatriene **5** incorporates vicinal diol stereocenters that are distant from the stereocenter to be formed. Exposure of imine **15** to 2.5 mol % of [RhCl(*coe*)₂]₂ and 5 mol % of the electron rich ligand 4-(diethylphosphino)-*N,N*-dimethylaniline at 65 °C led to highly selective formation of dihydropyridine **16** in excellent yield (84% by ¹H NMR analysis). While this tandem reaction was found not to be overly sensitive to concentration, reaction temperature is important, with higher temperatures resulting in lower yields and the formation of isomeric byproducts. Intermediate **16** was reduced without isolation using NaHB(OAc)₃ and AcOH

to provide tetrahydropyridine **17** in 65% overall yield and >20:1 *dr*, which thereby confirms the high torquoselectivity of the reaction.

To determine the origins of the torquoselectivity observed in the Rh(I)-catalyzed cascade sequence, computational studies of the key aza-electrocyclization were conducted using the ω B97x-D density functional with the 6-31+G(d,p) basis set. Table 1 illustrates the truncated substrates modeled computationally as well as the kinetic diastereoselectivities of ring closures of these compounds. The sense and level of torquoselectivities computed are consistent with experimental results. Discussion below of stereoiduction emphasizes the results of our computational studies of **E**, the 1-azatriene that most closely resembles the experimental substrate **5**.

The torquoselectivity of the electrocyclization is controlled by the transition state conformational preferences of the six-membered ring appended to the 1-azatriene. In the favored transition structure, **c-tsE**, the six-membered ring adopts a distorted chair-like arrangement, whereas this ring is forced into a twist boat arrangement in **tb-tsE**, destabilizing this transition structure by 3.2 kcal mol⁻¹. Arguments first proposed to rationalize electrophilic additions to cyclohexenes and their corresponding oxides¹⁵ can be extended to rationalize these conformational differences. The favored mode of disrotation forces C5 of the triene moiety to pyramidalize “downwards” (as shown in Figure 1) allowing the six-membered ring to adopt a chair-like conformation; pyramidalization of this carbon in the opposite direction is responsible for the twist-boat arrangement found in TSE2. This effect is likely general and could be exploited to perform diastereoselective electrocyclizations of similar chiral cyclic trienes.¹⁶

Figure 2 depicts the free energy surface of both modes of disrotatory electrocyclization as well as the reactant conformers of **E**. The global minimum conformer of **E** is **c-E1**, which features a chair-like six-membered ring and an s-trans arrangement of the azatriene moiety. **tb-E1** is 4.1 kcal mol⁻¹ in energy and leads to the disfavored transition structure. The helical arrangement of the azatriene in this structure forces the fused ring to adopt the less stable twist-boat conformation, demonstrating that the geometry required to form **tb-tsE** is inherently strained. The reactive conformers **c-E2** and **tb-E2** also differ in energy by approximately 4 kcal mol⁻¹, suggesting the magnitude of this conformational effect is similar in the ground and transition states.

With the concise asymmetric synthesis of intermediate **17** accomplished, the stage was set for completing the synthesis of *ent*-ketorfanol (**1**). The remaining tasks included cleavage of the silyl ether and ketal protecting groups, intramolecular Friedel–Crafts alkylation, and transformation of the diol to the desired ketone moiety. All of these steps could theoretically be accomplished under acidic conditions. We therefore attempted to carry out this sequence in a single step by subjecting **17** to phosphoric acid at elevated temperature, which resulted in a 2:1 inseparable mixture of **18** and *ent*-ketorfanol (**1**), favoring **18** in a combined 69% yield (Scheme 4). Under these strongly acidic conditions, rapid cleavage of the ketal and silyl protecting group occurs along with ionization to give the stabilized 2°/3° allylic carbocation **19**, which upon hydrogen migration affords ketone **20**. This ketone intermediate

accumulates as determined by NMR reaction monitoring. Subsequent intramolecular Friedel–Crafts alkylation of **20** then provides regioisomers **18** and **1**.

The poor regioselectivity of the Friedel–Crafts reaction was not unexpected but did pose a significant challenge. An effective solution to this problem would be to block the position *para* to the hydroxyl group on the aromatic ring. However, a silicon blocking group would not likely survive the strongly acidic conditions necessary for the Friedel–Crafts cyclization and a bromine blocking group would likely be incompatible with the C–H functionalization conditions due to competitive C–Br insertion.¹⁷ We therefore targeted a substrate with a chloride *para* to the hydroxy group (Scheme 5). Benzyl chloride **21** was readily coupled with terminal alkyne **12** according to our previously described alkynylation conditions. Transformation of the α,β -unsaturated ester **22** to the required imine **24** then proceeded without incident.

We were now ready to subject imine **24** to our Rh(I)-catalyzed C–H functionalization conditions (Scheme 6). At 55 °C within 3 h, dihydropyridine **25** was produced in excellent yield as a single diastereomer (>95:5 *dr*). Subsequent *in situ* reduction with NaHB(OAc)₃ provided tetrahydropyridine **26** in 69% isolated yield. Although the deactivating nature of the chloride substitution in **26** necessitated a higher temperature for the phosphoric acid mediated Friedel–Crafts alkylation as compared to the des-chloro compound, cyclization to **27** proceeded with excellent levels of regio- and diastereocontrol. Hydrodehalogenation¹⁸ of the aryl chloride in **27** with H₂ in the presence of Pd/C and NaHCO₃ cleanly afforded *ent*-ketorfanol (**1**). The structure and absolute configuration were rigorously established by x-ray crystallography.¹²

The asymmetric total synthesis of *ent*-ketorfanol has been accomplished in 11 steps and 9% overall yield from commercially available, achiral starting materials. In contrast, the only published routes to ketorfanol are through a multi-step degradation of morphine or naltrexone.³ The Rh(I)-catalyzed alkenylation/ 6π -electrocyclization cascade rapidly furnishes a bicyclic 1,2-dihydropyridine that serves as a key intermediate in the synthesis. The electrocyclization is highly torquoselective and thereby enables the use of a Sharpless asymmetric dihydroxylation to readily produce either enantiomer of ketorfanol. The acid-catalyzed tandem pinacol rearrangement/Friedel–Crafts alkylation not only provides the multicyclic drug framework but also in an efficient redox neutral process converts the diol that served as the stereocontrolling element to the requisite ketone moiety.

In previous reports, we have demonstrated the versatility of our Rh(I)-catalyzed C–H functionalization, electrocyclization, and reduction sequence for regio- and stereoselectively incorporating diverse substituents into tetrahydropyridines.^{5c–h} For this reason, the synthetic route reported here should enable the straightforward preparation of a variety of ketorfanol analogues and thus, provides an avenue for improving drug properties.

Supplementary Material

Refer to Web version on PubMed Central for supplementary material.

Acknowledgments

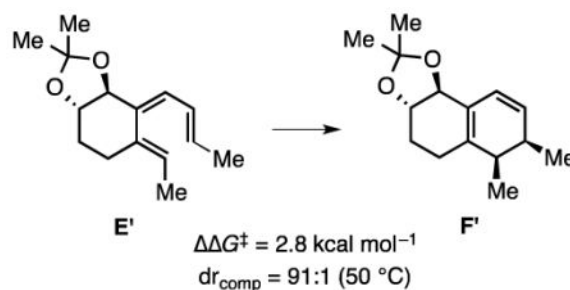
This work was supported by NIH Grant GM069559 (to J.A.E.). E.M.P. also acknowledges support from an NRSA postdoctoral fellowship (F32GM090661), and S.D. is grateful to the Swiss National Science Foundation for a postdoctoral fellowship (PBZHP2-130-966). We gratefully acknowledge Dr. Michael Takase for solving the crystal structures of **1**•HCl. We also acknowledge the financial support of the NIH (GM-36700 and CHE-1351104 to K.N.H.) A.P. thanks the Chemical-Biology Interface Training Program for its support (T32 GM 008496). A.P. acknowledges the University of California, Los Angeles for financial support. Density functional theory computations were performed using the Extreme Science and Engineering Discovery Environment (XSEDE)'s Gordon supercomputer (OCI-1053575) at the San Diego Supercomputing Center.

References

1. Typing the name of these drug and drug candidates into the NCGC Pharmaceutical Collection database provides compound structure, bioactivity, full list of literature, and access to ongoing clinical trials, applications, and usage.
2. a) Filizola M, Devi LA. *Nature*. 2012; 485:314–317. [PubMed: 22596150] b) Manglik A, Kruse AC, Kobilka TS, Thian FS, Mathiesen JM, Sunahara RK, Pardo L, Weis WI, Kobilka BK, Granier S. *Nature*. 2012; 485:321–326. [PubMed: 22437502] c) Wu HX, Wacker D, Mileni M, Katritch V, Han GW, Vardy E, Liu W, Thompson AA, Huang XP, Carroll FI, Mascarella SW, Westkaemper RB, Mosier PD, Roth BL, Cherezov V, Stevens RC. *Nature*. 2012; 485:327–332. [PubMed: 22437504] d) Granier S, Manglik A, Kruse AC, Kobilka TS, Thian FS, Weis WI, Kobilka BK. *Nature*. 2012; 485:400–404. [PubMed: 22596164]
3. For the synthesis of ketorfanol from the degradation of heavily functionalized natural product starting materials, see: Manmade A, Dalzell HC, Howes JF, Razdan RK. *J Med Chem*. 1981; 24:1437–1440. [PubMed: 7310820] Ida Y, Nemoto T, Hirayama S, Fujii H, Osa Y, Imai M, Nakamura T, Kanemasa T, Kato A, Nagase H. *Bioorg Med Chem*. 2012; 20:949–961. [PubMed: 22197670]
4. For reviews and leading references on syntheses of morphine and related natural products, see: Reed JW, Hudlicky T. *Acc Chem Res*. 2015; 48:674–687. [PubMed: 25730681] Rinner U, Hudlicky T. *Top Curr Chem*. 2012; 300:33–66. [PubMed: 21547687] Chida N. *Top Curr Chem*. 2011; 299:1–28. [PubMed: 21630507] Tissot M, Phipps RJ, Lucas C, Leon RM, Pace RDM, Ngouansavanh T, Gaunt MJ. *Angew Chem Int Ed*. 2014; 53:13498–13501. *Angew Chem*. 2014; 126:13716–13719. Ichiki M, Tanimoto H, Miwa S, Saito R, Sato T, Chida N. *Chem Eur J*. 2013; 19:264–269. [PubMed: 23180383] Li J, Liu GL, Zhao XH, Du JY, Qu H, Chu WD, Ding M, Jin CY, Wei MX, Fan CA. *Chem Asian J*. 2013; 8:1105–1109. [PubMed: 23509056] Varghese V, Hudlicky T. *Angew Chem Int Ed*. 2014; 53:4355–4358. *Angew Chem*. 2014; 126:4444–4447. Kimishima A, Umihara H, Mizoguchi A, Yokoshima S, Fukuyama T. *Org Lett*. 2014; 16:6244–6247. [PubMed: 25423610]
5. a) Colby DA, Bergman RG, Ellman JA. *J Am Chem Soc*. 2008; 130:3645–3651. [PubMed: 18302381] b) Duttwyler S, Lu C, Rheingold AL, Bergman RG, Ellman JA. *J Am Chem Soc*. 2012; 134:4064–4067. [PubMed: 22356093] c) Duttwyler S, Chen S, Takase MK, Wiberg KB, Bergman RG, Ellman JA. *Science*. 2013; 339:678–682. [PubMed: 23393259] d) Ischay MA, Takase MK, Bergman RG, Ellman JA. *J Am Chem Soc*. 2013; 135:2478–2481. [PubMed: 23398467] e) Duttwyler S, Chen S, Lu C, Mercado BQ, Bergman RG, Ellman JA. *Angew Chem Int Ed*. 2014; 53:3877–3880. *Angew Chem*. 2014; 126:3958–3961. f) Mesganaw T, Ellman JA. *Org Process Res Dev*. 2014; 18:1097–1104. [PubMed: 25288871] g) Mesganaw T, Ellman JA. *Org Process Res Dev*. 2014; 18:1105–1109. [PubMed: 25288872]
6. Intramolecular Friedel Crafts alkylation has been used to form this ring system, but not in the presence of the acid-labile allylic alcohol functionality. Grewe R, Mondon A. *Chem Ber*. 1948; 81:279–286.
7. For a discussion on redox economy in synthesis, see: Burns NZ, Baran PS, Hoffmann RW. *Angew Chem Int Ed*. 2009; 48:2854–2867. *Angew Chem*. 2009; 121:2896–2910.
8. For a recent review on asymmetric electrocyclization reactions, see: Thompson S, Coyne AG, Knipe PC, Smith MD. *Chem Soc Rev*. 2011; 40:4217–4231. [PubMed: 21566810]
9. a) Hsung RP, Wei LL, Sklenicka HM, Douglas CJ, McLaughlin MJ, Mulder JA, Yao LJ. *Org Lett*. 1999; 1:509–512. b) Tanaka K, Katsumura S. *J Am Chem Soc*. 2002; 124:9660–9661. [PubMed:

12175196] c) Sklenicka HM, Hsung RP, McLaughlin MJ, Wei LI, Gerasyuto AI, Brennessel WB. *J Am Chem Soc.* 2002; 124:10435–10442. [PubMed: 12197745] d) Sydorenko N, Hsung RP, Vera EL. *Org Lett.* 2006; 8:2611–2614. [PubMed: 16737326] e) Kobayashi T, Takeuchi K, Miwa J, Tsuchikawa H, Katsumura S. *Chem Commun.* 2009:3363–3365. f) Sakaguchi T, Kobayashi S, Katsumura S. *Org Biomol Chem.* 2011; 9:257–264. [PubMed: 21082129]

10. For recent reports of remote stereocontrol of triene electrocyclization, see: Ma ZX, Patel A, Houk KN, Hsung RP. *Org Lett.* 2015; 17:2138–2141. [PubMed: 25859907] Patel A, Barcan GA, Kwon O, Houk KN. *J Am Chem Soc.* 2013; 135:4878–4883. [PubMed: 23448287] Barcan GA, Patel A, Houk KN, Kwon O. *Org Lett.* 2012; 14:5388–5391. [PubMed: 23039026]
11. Xu DQ, Crispino GA, Sharpless KB. *J Am Chem Soc.* 1992; 114:7570–7571.
12. Synthetic details, characterization, and molecular structures obtained by X-ray structural analysis of compounds are described in the Supporting Information. CCDC 1404582 (**11**) and 1404583 (**1•HCl**) contain the supplementary crystallographic data for this paper. These data can be obtained free of charge from The Cambridge Crystallographic Data Centre via www.ccdc.cam.ac.uk/data_request/cif.
13. Davies KA, Abel RC, Wulff JE. *J Org Chem.* 2009; 74:3997–4000. [PubMed: 19422268]
14. Larsen CH, Anderson KW, Tundel RE, Buchwald SL. *Synlett.* 2006:2941–2946.
15. Fürst A, Plattner PA. *Hel Chim Acta.* 1949; 32:275–283.
16. Computations of the electrocyclic reaction of carbatriene analogue of **E** predict a similar level of torquoselectivity.



17. For a leading reference, see: Lewis JC, Berman AM, Bergman RG, Ellman JA. *J Am Chem Soc.* 2008; 130:2493–2500. [PubMed: 18251465]

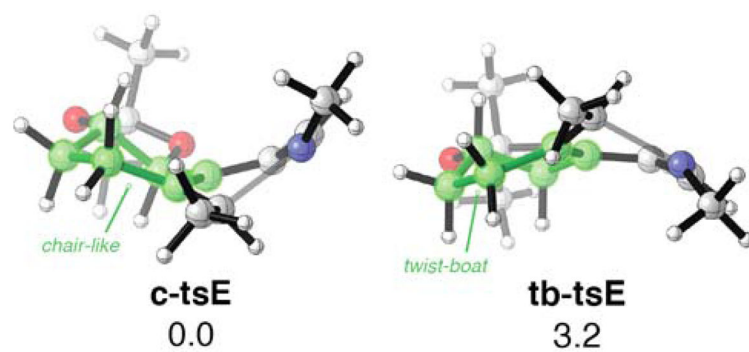


Figure 1. ω B97x-D/6-31+G(d,p)-optimized transition structures and their relative free energies (in kcal mol⁻¹).

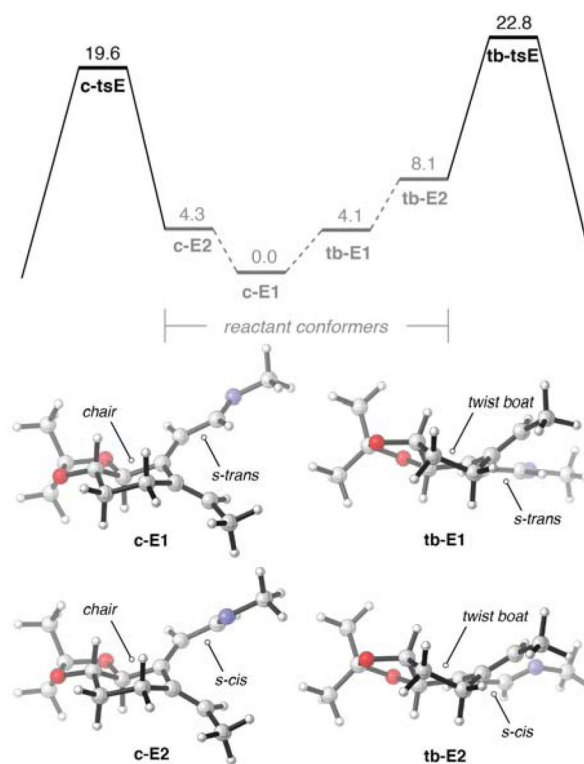
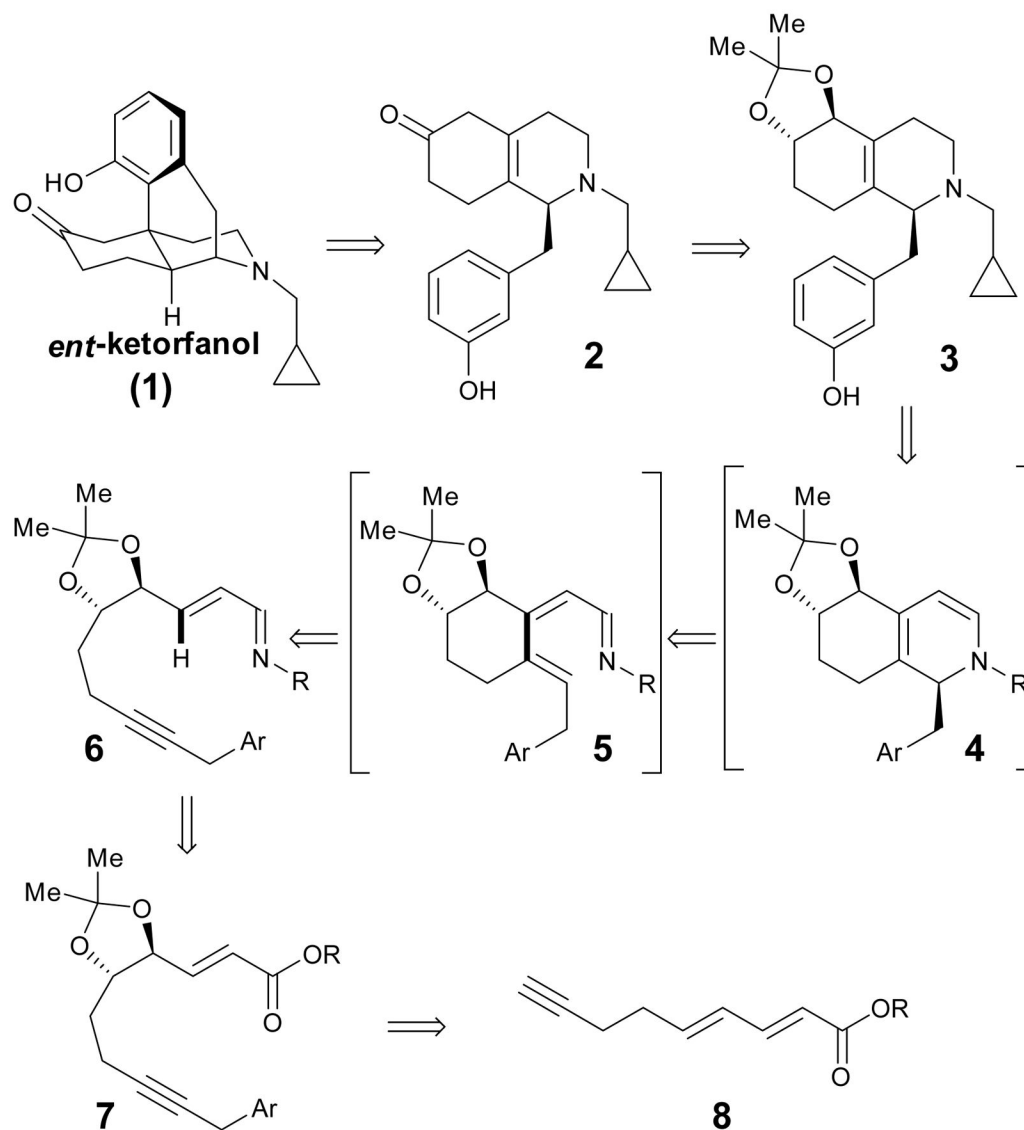
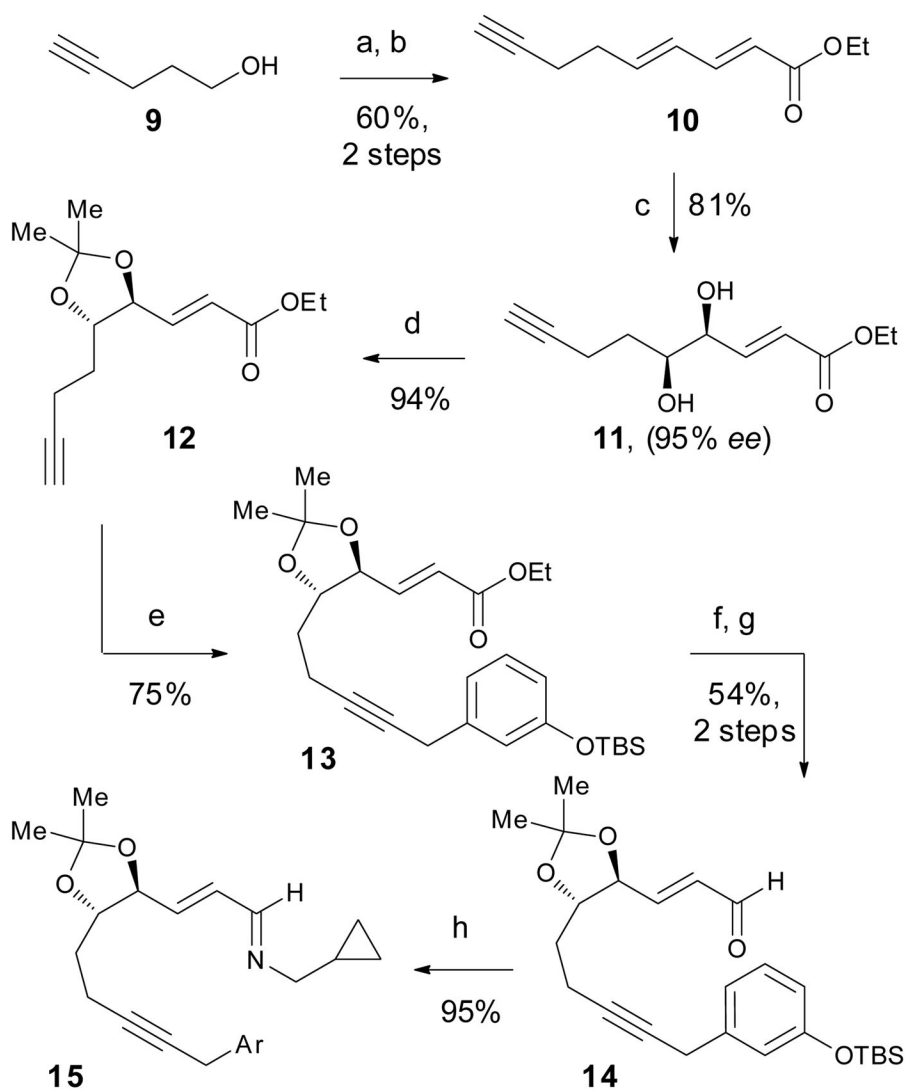


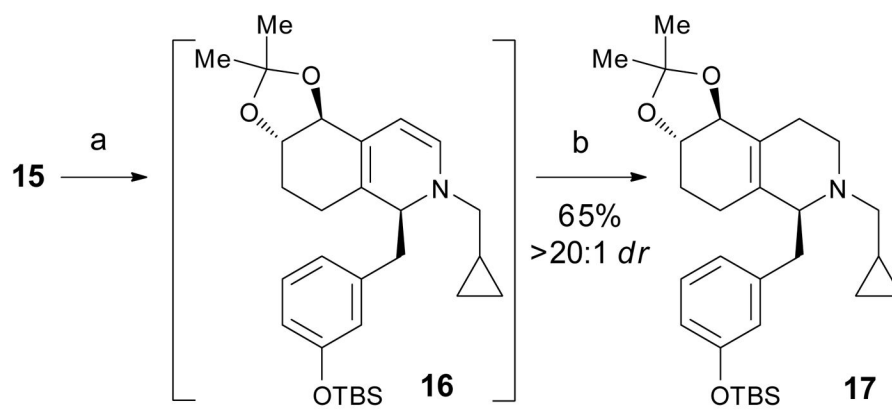
Figure 2. Free energy diagram of the electrocyclic ring closure of 1-aza-3,5-triene **E** and the computed structures of the reactant conformers of **E**. Free energies (in kcal mol⁻¹) and structures were determined using ω B97x-D/6-31+G(d,p).



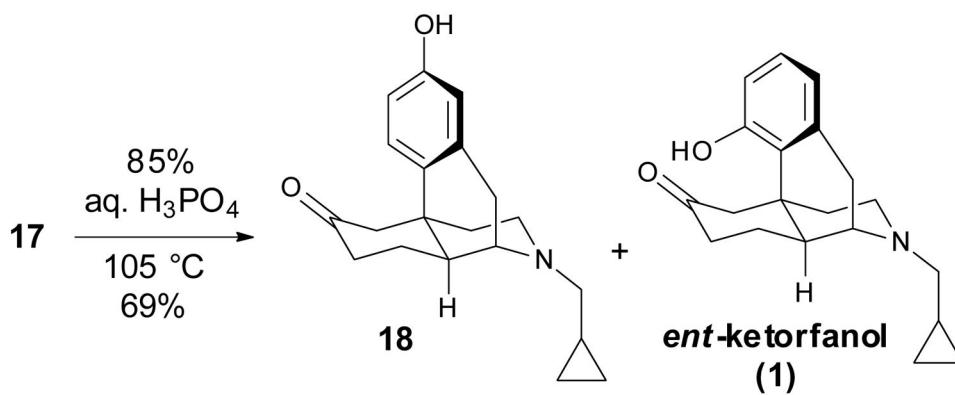
Scheme 1.
ent-Ketorfanol retrosynthesis.

**Scheme 2.**

Synthesis of imine **15**. Reagents and conditions: (a) $(\text{COCl})_2$, DMSO, Et_3N , CH_2Cl_2 , -78 °C; (b) $n\text{BuLi}$, $i\text{Pr}_2\text{NH}$, (*E*)-ethyl-4-(diethoxyphosphoryl)but-2-enoate, $-78 \rightarrow 0$ °C; (c) AD-mix- α , MeSO_2NH_2 , $t\text{BuOH}$, H_2O , 0 °C; (d) 2,2-dimethoxypropane, $p\text{TsOH}$ (10 mol %), CH_2Cl_2 , 0 °C; (e) 3-TBSOPh CH_2Cl , $\text{PdCl}_2(\text{CH}_3\text{CN})_2$ (5 mol %), XPhos (15 mol %), Cs_2CO_3 , THF, 65 °C; (f) DIBAL, CH_2Cl_2 , -78 °C; (g) Dess–Martin periodinane, pyridine, CH_2Cl_2 , 0 °C; (h) cyclopropylmethyl amine, toluene, 3Å MS .

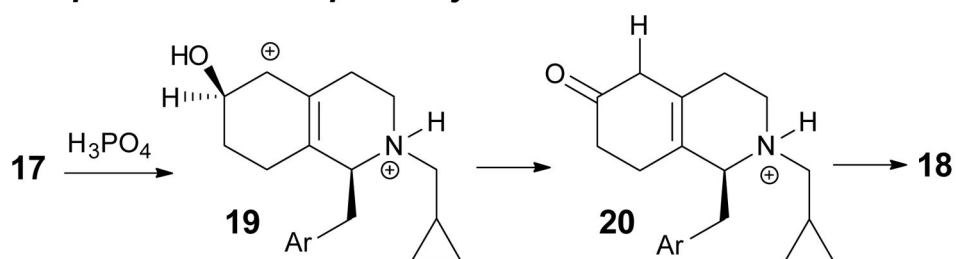
**Scheme 3.**

Rh(I)-catalyzed C–H insertion reaction. *Reagents and conditions:* (a) $[\text{RhCl}(\text{coe})_2]_2$ (2.5 mol %), 4-(diethylphosphino)-*N,N*-dimethylaniline (5 mol %), toluene, 65 °C; (b) $\text{NaHB}(\text{OAc})_3$, AcOH, EtOH, 0 \rightarrow 23 °C.



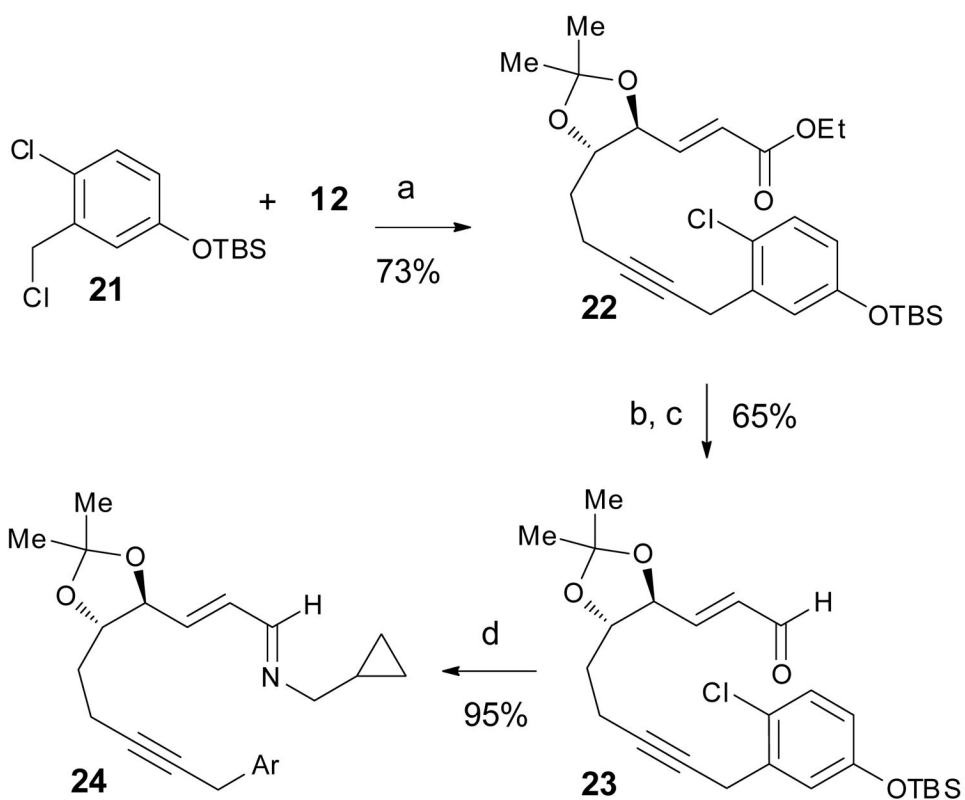
2:1 regioisomers

Proposed reaction pathway

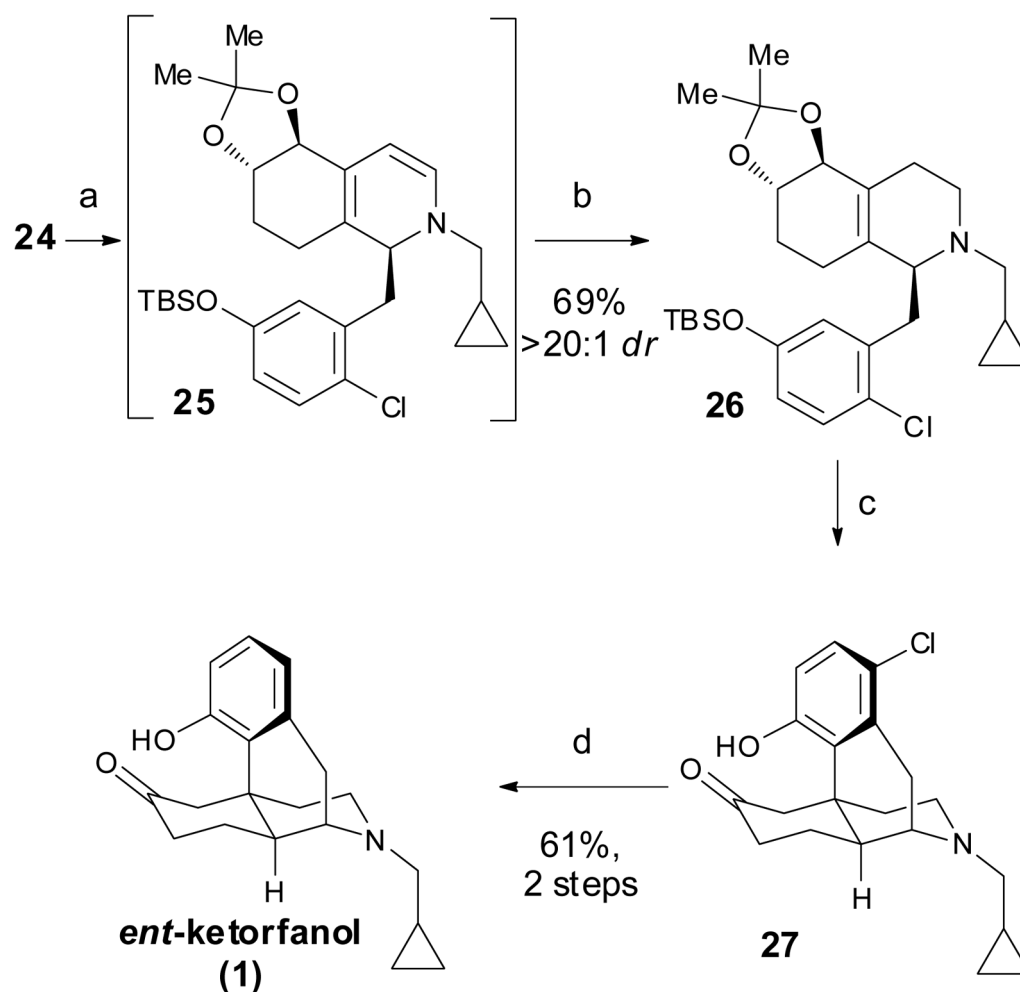


Scheme 4.

Intramolecular Friedel–Crafts alkylation with concomitant redox neutral diol to ketone interconversion.

**Scheme 5.**

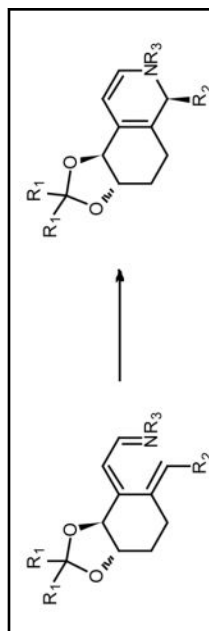
Synthesis of imine **24**. *Reagents and conditions:* (a) $\text{PdCl}_2(\text{CH}_3\text{CN})_2$ (5 mol %), XPhos (15 mol %), Cs_2CO_3 , THF, 65 °C; (b) DIBAL, THF, -78 °C; (c) Dess–Martin periodinane, pyridine, CH_2Cl_2 , 0 °C; (d) cyclopropylmethyl amine, toluene, 3 Å MS.

**Scheme 6.**

Synthesis of *ent*-ketorfanol (**1**). *Reagents and conditions:* (a) $[\text{RhCl}(\text{coe})_2]_2$ (5 mol %), 4-(diethylphosphino)-*N,N*-dimethylaniline (10 mol %), toluene, 55 °C; (b) $\text{NaHB}(\text{OAc})_3$, AcOH, EtOH, 0 \rightarrow 23 °C; (c) 85% phosphoric acid, 125 °C; (d) H_2 , Pd/C, NaHCO_3 , EtOH.

1-Aza-3,5-trienes modeled computationally, computed activation free energies differences, and computed torquoselectivities.

Table 1



Compound	R ₁	R ₂	R ₃	G [‡] (kcal/mol)	Torquoselectivity ^a
A	H	H	H	3.1	187:1
B	H	Me	H	3.3	262:1
C	Me	Me	H	3.6	435:1
D	H	Me	Me	3.1	187:1
E	Me	Me	Me	3.2	221:1

^aFree energies and torquoselectivities determined assuming a standard state of 1 atm and 298.15 K.